

## Feasibility of Abdominal MRI at 7.0 T Using a Novel 32 Channel Transceiver Coil Array

Fabian Hezel<sup>1</sup>, Andreas Gräßl<sup>1</sup>, Peter Kellman<sup>2</sup>, and Thoralf Niendorf<sup>1,3</sup>

<sup>1</sup>Berlin Ultrahigh Field Facility, MDC Berlin, Berlin, Germany, <sup>2</sup>Laboratory of Cardiac Energetics, National Institutes of Health/NHLBI, Bethesda, MD, United States,

<sup>3</sup>Experimental and Clinical Research Center (ECRC), Charité Campus Buch, Humboldt-University, Berlin, Germany

**Introduction:** Abdominal imaging examinations constitute a growing fraction of clinical MRI exams [1]. Since ultrahigh field magnetic resonance imaging becomes more widespread, a range of applications established in the clinical scenario at 1.5 T and 3.0 T is in the research spotlight at 7.0 T. This includes explorations into abdominal imaging with the ultimate goal to put the intrinsic sensitivity advantage at 7T into clinical use. Arguably, abdominal MRI at 7.0 T earns the moniker of “advanced MR applications” since some of the inherent advantages of ultrahigh-field MRI might be offset by practical constraints associated with RF power deposition limits, dielectric effects and momentary RF non-uniformities. Therefore, transmit-receive (TX/RX) coil array designs are not a novelty but a necessity for ultrahigh field abdominal MR to tackle the challenge of  $B_{1+}$ -field inhomogeneities. For all these reasons, this work proposes a 32 channel TX/RX body coil array and examines its feasibility for abdominal imaging at 7.0 T using  $T_1$ -weighted ultrahigh resolution imaging, fat/water separated imaging and  $T_2^*$  mapping in this pilot study.

**Methods:** Volunteer experiments were performed on a 7.0 T whole body MR system (Magnetom, Siemens, Erlangen, Germany) together with a dedicated 32-element TX/RX body coil array. The coil array consists of planar (posterior section) and bend(anterior section) modules. Each module comprises 4 independent transceiver loop elements ( $2 \times 2$  array) with an rectangular size of 6 cm x 6 cm each and a conductor width of 1 cm. Adjacent elements share a common conductor with an integrated, adjustable capacitor for decoupling of neighboring elements. For the proposed 32 channel TX/RX design four planar modules and four bend modules are realized as shown in Fig.1. High resolution  $T_1$  weighted imaging was performed using a GRE technique. Imaging parameters were set to: slice thickness=2.5 mm, nominal flip angle= 38°, acquisition matrix 800 x 1024, TR/TE = 21/3.08 ms, bandwidth= 380Hz/pixel. A multi-echo GRE technique was applied for fat/water separation. A multi-shot approach was used to reduce the effective echo spacing by interleaving. For this purpose 4 echoes with an echo spacing of 0.25 ms were used. Water-fat separated image reconstruction used a multi-echo Dixon like technique based on the VARPRO formulation with graphcut optimization to jointly estimate the water, fat [2]. For  $T_2^*$  mapping 8 echoes were acquired in-phase with an echo spacing of 1.02 ms. Images were processed with MATLAB (Mathworks, Natick, MA, USA) applying a mono-exponential fitting pixel-by-pixel  $T_2^*$  quantification. First and second order shimming was applied for a rectangular region encompassing the liver.

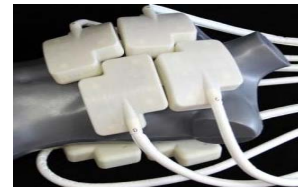


Fig.1: 32 channel RX/TX coil placed on a mannequin

**Results:** Fig.2a illustrates the overall image quality for a central coronal slices using gradient echo imaging. The coil arrays sensitivity profile was found to be suitable for a anatomic coverage of 35 cm along the superior-inferior direction.  $T_1$  weighted images delivered high contrast between vessel and parenchyma without the need of contrast agent application as demonstrated in Fig.2b and 3b. It should be noted that significant RF shading occurred in deep lying liver regions, although various phase settings were applied for the anterior and posterior sections of the 32 channel TX/RX array (Fig.3a) to improve the  $B_{1+}$  uniformity. High details of subtle liver structures can be observed as illustrated by the zoomed versions of the high spatial resolution images. Besides great vessels, capillaries in the dimension of half a millimeter of diameter were clearly identifiable due to the superb spatial resolution of  $(0.3 \times 0.3 \times 2.5) \text{ mm}^3$  which is superior to that commonly achieved in clinical settings at 1.5 T and 3.0 T. Abdominal fat/water imaging at 7.0 T was found to be challenging due to (i)  $B_0$  variations which are more pronounced at 7.0 T vs. lower field strengths, (ii)  $T_2$  dephasing, and (iii) larger chemical shift. Hence, a multi-shot approach was used to achieve shorter echo spacing. Decreased slice thickness was used to reduce  $T_2^*$  losses. Fat and water were correctly classified as demonstrated in Fig. 4 and good separation was achieved across the full field of view.  $B_0$  uniformity was found to be clinically acceptable as indicated by the  $T_2^*$  map shown in Figure 5. Using a multi-echo approach  $T_2^*$  was found to be approximately  $10.4 \pm 1.7$  ms for the parenchyma and approximately 20 ms for the large liver blood vessels.

**Discussion and Conclusions:** Despite the observed non-uniformities of the RF field distribution, our preliminary results suggest that high spatial resolution anatomic details accomplished at 7.0 T can be considered to be beneficial clinical liver imaging. As transmit array hardware becomes more readily available, 7.0 T MRI may be expected to transition into an enabling technology for high spatial resolution abdominal imaging. However, further clinical studies have to be conducted carefully to validate the diagnostic capability of 7.0 T liver imaging versus established abdominal imaging protocols used in day-to-day clinical routine at 1.5T or 3.0 T.

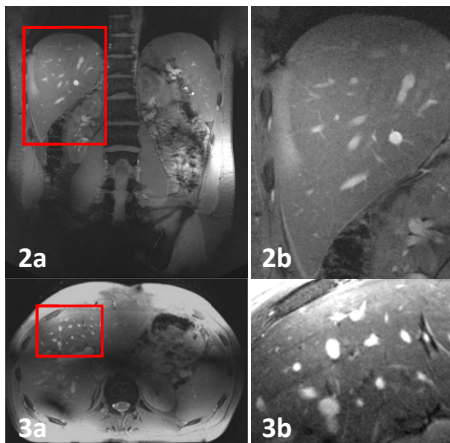


Fig.2: a)  $T_1$  weighted images of a central coronal abdominal slice derived from gradient echo imaging using a voxel size of  $(0.4 \times 0.4 \times 2.5) \text{ mm}^3$  b) zoomed view of the area marked in red in Fig.2a

Fig.3: a)  $T_1$  weighted axial slice across the liver derived from gradient echo imaging using a spatial resolution of  $(0.3 \times 0.3 \times 2.5) \text{ mm}^3$ . No contrast agent was applied. b) Zoomed view of the region marked in red in Fig.3a. Subtle anatomic liver structures are clearly identifiable including capillaries in with a diameter as small as of 0.5 mm

Fig.4: Coronal slice used for fat/ water separated imaging. a) water only image and b) fat only image demonstrates the fat/water separation and suppression across the FOV

Fig.5: Abdominal  $T_2^*$  map of a coronal slice showing a rather uniform  $T_2^*$  distribution over the liver

**References:** [1] M. M. Barth et al, “Body MR Imaging at 3.0 T: Understanding the Opportunities and Challenges,” *Radiographics*, vol. 27, no. 5, pp. 1445-1462, Oct. 2007. [2] D. Hernando et al, “Chemical shift-based water/fat separation: a comparison of signal models,” *MRM*, vol. 64, no. 3, pp. 811-822, Sep. 2010.